

## Supplemental Data

### **PINCH1 controls Akt1 for regulating radiation sensitivity by inhibiting PP1 $\alpha$**

Iris Eke, Ulrike Koch, Stephanie Hehlhans, Veit Sandfort, Fabio Stanchi, Daniel Zips, Michael Baumann, Anna Shevchenko, Christian Pilarsky, Michael Haase, Gustavo B. Baretton, Véronique Calleja, Banafshé Larijani, Reinhard Fässler, and Nils Cordes

### Supplemental Methods

*Cell culture, radiation exposure and 2D and 3D colony formation assay.* Cells were cultured in Dulbecco's Modified Eagle Medium (PAA; plus glutamax-I) supplemented with 10% fetal calf serum (Biochrom) and 1% non-essential amino acids (PAA) (1). Single doses of 200 kV X-rays (Yxlon Y.TU 320; Yxlon; 0.5 mm copper filter; ~1.3 Gy/min, 20 mA) were applied and measured using a Duplex dosimeter (PTW) (1). To evaluate two(2D)- or three(3D)-dimensional clonogenic cell survival, we plated cells on or in laminin-rich extracellular matrix (lrECM (Matrigel™); BD) as published (1).

*Antibodies.* anti-GSK3 $\beta$ , anti-PINCH1, anti-CD31 (BD), anti-Akt1, anti-pAkt1 S473, anti-pAkt1 T308, anti-FoxO1, anti-pFoxO1 S256 (detects pFoxO1 S256 and pFoxO4 S197), anti-FoxO4, anti-pGSK3 $\beta$  S9, anti-pGSK3 $\alpha/\beta$  S21/9, anti-ILK (Cell Signaling), anti- $\beta$ -actin (Sigma), anti-GFP, anti-PPP1A (Abcam), anti-Ki-67 (Dako), rabbit polyclonal anti-Pimonidazole (kindly provided by J. Raleigh, University of North Carolina, USA); HRP-conjugated donkey anti-rabbit and sheep anti-mouse secondary antibodies (Amersham), goat anti-rat TRITC and goat anti-rabbit FITC (Jackson ImmunoResearch), Alexa Fluor<sup>®</sup> 594 goat anti-rabbit IgG (Invitrogen).

*Akt1 kinase assay.* Akt1 kinase assay was performed according to the manufacturer's protocol (Cell Signaling) (1).

*Akt1* or *PINCH1* knockdown. *Akt1* and *PINCH1* siRNA target sequences (Applied Biosystems):

siRNA	Sequence (Sense)	siRNA ID
mAkt1 siRNA #1	5'-GGUAAUUCGAUGAGGAGUUtt-3'	#65681
mAkt1 siRNA #2	5'-GCACCGUGUGACCAUGAACtt-3'	#162426
hAkt1 siRNA #1	5'-GGGCACUUUCGGCAAGGUGtt-3'	#633
hAkt1 siRNA #2	5'-GGCUCCCCUCACAACUUCtt-3'	#42811
mPINCH1 siRNA #1	5'-CGAACAGUGCUUCGUUAUGUtt-3'	#172029
mPINCH1 siRNA #2	5'-GGGCUUGGCCUACUGUGAAtt-3'	#172030
hPINCH1 siRNA #1	5'-GGACCUAUAUGAAUGGUUUtt-3'	#15687
hPINCH1 siRNA #2	5'-GCUAUAUCUCAAGCAGUUtt-3'	#289501

Non-specific control siRNA: 5'-GCAGCUAUAUGAAUGUUGUtt-3' (MWG). siRNA delivery was accomplished as published (2). Forty-eight hours after transfection cells were either irradiated (colony formation assay) or lysed for Western blotting.

#### *PINCH1* expression constructs and site-directed mutagenesis

Specific primers used:

Primer	Sequence
PINCH1-C1-fw	5'-gg-GGTACC-CTGGGCGTGGCGGCCGGAA-3'
PINCH1-C1-rev	5'-cg-GGATCC-TTATTTCCCTCCTAAGGTCTCAG-3'
PINCH1-C1-LIM5	5'-cg-GGATCC-T-CAAACATCACCAAACAGCTGATTA-3'
PINCH1-KFAEA-fw	5'-CACACTCAAGAATAAATTTGCGGAAGCTGACATGAAGCCAGTCTG-3'
PINCH1-KFAEA-rev	5'-CAGACTGGCTTCATGTCAGCTTCCGCAAATTTATTCTTGAGTGTG-3'
PINCH1-AFAEA-fw	5'-CTCACACTCAAGAATGCATTTGCGGAAGCTGACATGAAGCCAGTCTG-3'
PINCH1-AFAEA-rev	5'-CAGACTGGCTTCATGTCAGCTTCCGCAAATGCATTCTTGAGTGTGAG-3'

*Transfection of Akt1 and PINCH1 plasmids.* Cells were transiently transfected with different RFP-Akt1 vectors (wt, S473D/T308D, S473A, S473A/T308A,  $\Delta$ PH) (3) or EGFP-PINCH1 expression constructs as published (4).

*Mass spectrometry.* IPI database was used as described (5).

*Sequence homology search.* Sequence homology search for the KFVEF motif in the PINCH1 protein sequence was performed (*Homo sapiens* Acc.No. NP\_004978, *Pan troglodytes* Acc.No.

XP\_001136475, *Xenopus laevis* Acc.No. ABS17667, *Danio rerio* Acc.No. NP\_001019560, *Mus*

*musculus* Acc.No. NP\_080424, *Equus caballus* Acc.No. XP\_001501201, *Rattus norvegicus* Acc.No.

XP\_574766, *Gallus gallus* Acc.No. NP\_001001766) using:

<http://bioinfo.genotoul.fr/multalin/multalin.html>; <http://esprpt.ibcp.fr/ESPrpt/ESPrpt/index.php>.

*Immunoprecipitation.* Immunoprecipitation was performed as described (1).

*Immunofluorescence staining.* Immunofluorescence staining was performed and fluorescence images were acquired as described (4).

*Identification of allografts in vivo.* PCR genotyping and PINCH1 protein expression of tumors was performed as described (6).

*Evaluation of local tumor control.* Actuarial estimates for time to local tumor recurrence were obtained using the Kaplan-Meier method and compared using Log rank test (GraphPad Prism software 4.03). For analysis of local tumor control data, censored animals were taken into account according to the method described by Walker and Suit (7). Tumor control data were fitted to the Poisson dose-response model. Tumor control probability (TCP) for a radiation dose 'D' is

$$TCP = \exp \left[ -N \cdot \exp \left( \ln n - \frac{D}{D_0} \right) \right]$$

where 'N' is the number of tumor stem cells at the start of treatment, 'n' is the "extrapolation" number in the two component cell survival model, and 'D<sub>0</sub>' is a parameter describing the sensitivity of tumor stem cells to irradiation. The tumor control dose 50% is derived from

$$TCD_{50} = D_0(\ln Nn + 0.367).$$

Model parameters were estimated by maximum likelihood analysis. The non-parametric bootstrap method was used to determine 95% confidence intervals for TCD<sub>50</sub>. All calculations were performed using the STATA/SE 8.0 software (STATA Corporation) (8).

*Histology.* Methods to assess vasculature, hypoxia and perfusion in transplanted tumors have been described previously (7, 9). The hypoxic marker Pimonidazole (Natural Pharmacia International) was injected i.p. (0.1 mg/g body weight, dissolved at 10 mg/ml in 0.9% NaCl) 1 hour before tumor excision and the perfusion marker Hoechst 33342 (0.05 ml/mouse, dissolved at 6 mg/ml in PBS; Sigma) was injected into the tail vein 1 minute before tumor excision (Figure S4A). After excision, tumors were cut into halves. One half was shock frozen in liquid nitrogen and stored at -80°C and the other half was fixed in formalin and embedded in paraffin. Frozen central whole tumor cross-sections were air dried at room temperature for 1 hour, then fixed in ice-cold acetone for 10 minutes, air dried, and rehydrated in PBS. One section per tumor was simultaneously incubated overnight with anti-mouse CD31 monoclonal antibody (blood vessels) and rabbit polyclonal anti-Pimonidazole antibody (hypoxia). Goat anti-rat TRITC and goat anti-rabbit FITC were used as secondary antibodies (controls were secondary antibodies only). For immunofluorescence, whole tumor cross-sections were scanned sequentially for Hoechst 33342, TRITC and FITC fluorescence at 100-fold magnification using a Zeiss Axioplan 2 fluorescence microscope (Carl Zeiss) equipped with a scanning stage (Maerzhäuser) and a digital camera (AxioCam MRm; Carl Zeiss), resulting in congruent digital images consisting of 110 - 240 visual fields per image. The scanning process and the subsequent image analysis were performed using the KS300 image analysis software (Kontron Elektronik). After scanning of the fluorescence signals, the sections were stained with hematoxyline and eosine (H&E). Binary images from the blinded samples were created by one investigator (U.K.) defining segmentation thresholds interactively considering signal-background intensity. A typical staining pattern for blood vessels (CD31) and for hypoxia (Pimonidazole) was found in all tumor sections. The procedure of threshold setting is arbitrary but reproducible (7). After scanning, the total tumor area and necrotic area were delineated with the computer mouse. The relative vascular area and Pimonidazole hypoxic fraction were determined as the CD31 and Pimonidazole positive area per viable tumor area, respectively. The fraction of perfused vessels was calculated from the ratio of CD31 staining overlapping with the Hoechst 33342 perfusion signal in 6 *PINCH1<sup>fl/fl</sup>* and 8 *PINCH1<sup>-/-</sup>* tumors, respectively. Moreover, we performed immunohistochemistry (Animal Research Peroxidase Kit; Dako) by staining paraffin embedded tumors (6 *PINCH1<sup>fl/fl</sup>* and 6 *PINCH1<sup>-/-</sup>* tumors) with anti-Ki-67 antibodies. The index for Ki-67 staining was determined in 10 randomly selected high-power fields (400-fold magnification) per

tumor. For evaluation of the histological parameters, mean values, standard deviation were calculated and compared using the unpaired, 2-sided t-test (GraphPad Prism software 4.03).

## Supplemental References

(Methodology without Microarray analysis)

1. Hehlhans, S., Eke, I., Deuse, Y., and Cordes, N. 2008. Integrin-linked kinase: dispensable for radiation survival of three-dimensionally cultured fibroblasts. *Radiother. Oncol.* 86:329-335.
2. Cordes, N., Seidler, J., Durzok, R., Geinitz, H., and Brakebusch, C. 2006. beta1-integrin-mediated signaling essentially contributes to cell survival after radiation-induced genotoxic injury. *Oncogene* 25:1378-1390.
3. Calleja, V., Alcor, D., Laguerre, M., Park, J., Vojnovic, B., Hemmings, B.A., Downward, J., Parker, P.J., and Larijani, B. 2007. Intramolecular and intermolecular interactions of protein kinase B define its activation in vivo. *PLoS Biol.* 5:e95.
4. Eke, I., Sandfort, V., Storch, K., Baumann, M., Roper, B., and Cordes, N. 2007. Pharmacological inhibition of EGFR tyrosine kinase affects ILK-mediated cellular radiosensitization in vitro. *Int. J. Radiat. Biol.* 83:793-802.
5. Kersey, P.J., Duarte, J., Williams, A., Karavidopoulou, Y., Birney, E., and Apweiler, R. 2004. The International Protein Index: an integrated database for proteomics experiments. *Proteomics* 4:1985-1988.
6. Li, S., Bordoy, R., Stanchi, F., Moser, M., Braun, A., Kudlacek, O., Wewer, U.M., Yurchenco, P.D., and Fassler, R. 2005. PINCH1 regulates cell-matrix and cell-cell adhesions, cell polarity and cell survival during the peri-implantation stage. *J. Cell Sci.* 118:2913-2921.
7. Yaromina, A., Zips, D., Thames, H.D., Eicheler, W., Krause, M., Rosner, A., Haase, M., Petersen, C., Raleigh, J.A., Quennet, V., et al. 2006. Pimonidazole labelling and response to fractionated irradiation of five human squamous cell carcinoma (hSCC) lines in nude mice: the need for a multivariate approach in biomarker studies. *Radiother. Oncol.* 81:122-129.
8. Yaromina, A., Krause, M., Thames, H., Rosner, A., Krause, M., Hessel, F., Grenman, R., Zips, D., and Baumann, M. 2007. Pre-treatment number of clonogenic cells and their radiosensitivity are major determinants of local tumour control after fractionated irradiation. *Radiother. Oncol.* 83:304-310.
9. Zips, D., Eicheler, W., Geyer, P., Hessel, F., Dorfler, A., Thames, H.D., Haberey, M., and Baumann, M. 2005. Enhanced susceptibility of irradiated tumor vessels to vascular endothelial growth factor receptor tyrosine kinase inhibition. *Cancer Res.* 65:5374-5379.

## Supplemental References

(Microarray analysis)

### Adrenal

Giordano, T.J., Thomas, D.G., Kuick, R., Lizyness, M., Misek, D.E., Smith, A.L., Sanders, D., Aljundi, R.T., Gauger, P.G., Thompson, N.W., et al. 2003. Distinct transcriptional profiles of adrenocortical tumors uncovered by DNA microarray analysis. *Am J Pathol* 162:521-531.

### Brain

Bredel, M., Bredel, C., Juric, D., Harsh, G.R., Vogel, H., Recht, L.D., and Sikic, B.I. 2005. Functional network analysis reveals extended gliomagenesis pathway maps and three novel MYC-interacting genes in human gliomas. *Cancer Res* 65:8679-8689.

Liang, Y., Diehn, M., Watson, N., Bollen, A.W., Aldape, K.D., Nicholas, M.K., Lamborn, K.R., Berger, M.S., Botstein, D., Brown, P.O., et al. 2005. Gene expression profiling reveals molecularly and clinically distinct subtypes of glioblastoma multiforme. *Proc Natl Acad Sci U S A* 102:5814-5819.

Shai, R., Shi, T., Kremen, T.J., Horvath, S., Liao, L.M., Cloughesy, T.F., Mischel, P.S., and Nelson, S.F. 2003. Gene expression profiling identifies molecular subtypes of gliomas. *Oncogene* 22:4918-4923.

Sun, L., Hui, A.M., Su, Q., Vortmeyer, A., Kotliarov, Y., Pastorino, S., Passaniti, A., Menon, J., Walling, J., Bailey, R., et al. 2006. Neuronal and glioma-derived stem cell factor induces angiogenesis within the brain. *Cancer Cell* 9:287-300.

### Breast

Finak, G., Bertos, N., Pepin, F., Sadekova, S., Souleimanova, M., Zhao, H., Chen, H., Omeroglu, G., Meterissian, S., Omeroglu, A., et al. 2008. Stromal gene expression predicts clinical outcome in breast cancer. *Nat Med* 14:518-527.

Radvanyi, L., Singh-Sandhu, D., Gallichan, S., Lovitt, C., Pedyczak, A., Mallo, G., Gish, K., Kwok, K., Hanna, W., Zubovits, J., et al. 2005. The gene associated with trichorhinophalangeal syndrome in humans is overexpressed in breast cancer. *Proc Natl Acad Sci U S A* 102:11005-11010.

Richardson, A.L., Wang, Z.C., De Nicolo, A., Lu, X., Brown, M., Miron, A., Liao, X., Iglehart, J.D., Livingston, D.M., and Ganesan, S. 2006. X chromosomal abnormalities in basal-like human breast cancer. *Cancer Cell* 9:121-132.

Turashvili, G., Bouchal, J., Baumforth, K., Wei, W., Dziechciarkova, M., Ehrmann, J., Klein, J., Fridman, E., Skarda, J., Srovnal, J., et al. 2007. Novel markers for differentiation of lobular and ductal invasive breast carcinomas by laser microdissection and microarray analysis. *BMC Cancer* 7:55.

## Colon

- Graudens, E., Boulanger, V., Mollard, C., Mariage-Samson, R., Barlet, X., Gremy, G., Couillault, C., Lajemi, M., Piatier-Tonneau, D., Zaborski, P., et al. 2006. Deciphering cellular states of innate tumor drug responses. *Genome Biol* 7:R19.
- Ki, D.H., Jeung, H.C., Park, C.H., Kang, S.H., Lee, G.Y., Lee, W.S., Kim, N.K., Chung, H.C., and Rha, S.Y. 2007. Whole genome analysis for liver metastasis gene signatures in colorectal cancer. *Int J Cancer* 121:2005-2012.
- Notterman, D.A., Alon, U., Sierk, A.J., and Levine, A.J. 2001. Transcriptional gene expression profiles of colorectal adenoma, adenocarcinoma, and normal tissue examined by oligonucleotide arrays. *Cancer Res* 61:3124-3130.
- Zou, T.T., Selaru, F.M., Xu, Y., Shustova, V., Yin, J., Mori, Y., Shibata, D., Sato, F., Wang, S., Oлару, A., et al. 2002. Application of cDNA microarrays to generate a molecular taxonomy capable of distinguishing between colon cancer and normal colon. *Oncogene* 21:4855-4862.

## Esophagus

- Hao, Y., Triadafilopoulos, G., Sahbaie, P., Young, H.S., Omary, M.B., and Lowe, A.W. 2006. Gene expression profiling reveals stromal genes expressed in common between Barrett's esophagus and adenocarcinoma. *Gastroenterology* 131:925-933.
- Kimchi, E.T., Posner, M.C., Park, J.O., Darga, T.E., Kocherginsky, M., Karrison, T., Hart, J., Smith, K.D., Mezhir, J.J., Weichselbaum, R.R., et al. 2005. Progression of Barrett's metaplasia to adenocarcinoma is associated with the suppression of the transcriptional programs of epidermal differentiation. *Cancer Res* 65:3146-3154.
- Wang, S., Zhan, M., Yin, J., Abraham, J.M., Mori, Y., Sato, F., Xu, Y., Oлару, A., Berki, A.T., Li, H., et al. 2006. Transcriptional profiling suggests that Barrett's metaplasia is an early intermediate stage in esophageal adenocarcinogenesis. *Oncogene* 25:3346-3356.

## Kidney

- Gumz, M.L., Zou, H., Kreinest, P.A., Childs, A.C., Belmonte, L.S., LeGrand, S.N., Wu, K.J., Luxon, B.A., Sinha, M., Parker, A.S., et al. 2007. Secreted frizzled-related protein 1 loss contributes to tumor phenotype of clear cell renal cell carcinoma. *Clin Cancer Res* 13:4740-4749.
- Higgins, J.P., Shinghal, R., Gill, H., Reese, J.H., Terris, M., Cohen, R.J., Fero, M., Pollack, J.R., van de Rijn, M., and Brooks, J.D. 2003. Gene expression patterns in renal cell carcinoma assessed by complementary DNA microarray. *Am J Pathol* 162:925-932.
- Lenburg, M.E., Liou, L.S., Gerry, N.P., Frampton, G.M., Cohen, H.T., and Christman, M.F. 2003. Previously unidentified changes in renal cell carcinoma gene expression identified by parametric analysis of microarray data. *BMC Cancer* 3:31.

## Lung

- Beer, D.G., Kardia, S.L., Huang, C.C., Giordano, T.J., Levin, A.M., Misek, D.E., Lin, L., Chen, G., Gharib, T.G., Thomas, D.G., et al. 2002. Gene-expression profiles predict survival of patients with lung adenocarcinoma. *Nat Med* 8:816-824.
- Bhattacharjee, A., Richards, W.G., Staunton, J., Li, C., Monti, S., Vasa, P., Ladd, C., Beheshti, J., Bueno, R., Gillette, M., et al. 2001. Classification of human lung carcinomas by mRNA expression profiling reveals distinct adenocarcinoma subclasses. *Proc Natl Acad Sci U S A* 98:13790-13795.
- Garber, M.E., Troyanskaya, O.G., Schluens, K., Petersen, S., Thaesler, Z., Pacyna-Gengelbach, M., van de Rijn, M., Rosen, G.D., Perou, C.M., Whyte, R.I., et al. 2001. Diversity of gene expression in adenocarcinoma of the lung. *Proc Natl Acad Sci U S A* 98:13784-13789.
- Powell, C.A., Spira, A., Derti, A., DeLisi, C., Liu, G., Borczuk, A., Busch, S., Sahasrabudhe, S., Chen, Y., Sugarbaker, D., et al. 2003. Gene expression in lung adenocarcinomas of smokers and nonsmokers. *Am J Respir Cell Mol Biol* 29:157-162.
- Stearman, R.S., Dwyer-Nield, L., Zerbe, L., Blaine, S.A., Chan, Z., Bunn, P.A., Jr., Johnson, G.L., Hirsch, F.R., Merrick, D.T., Franklin, W.A., et al. 2005. Analysis of orthologous gene expression between human pulmonary adenocarcinoma and a carcinogen-induced murine model. *Am J Pathol* 167:1763-1775.
- Su, L.J., Chang, C.W., Wu, Y.C., Chen, K.C., Lin, C.J., Liang, S.C., Lin, C.H., Whang-Peng, J., Hsu, S.L., Chen, C.H., et al. 2007. Selection of DDX5 as a novel internal control for Q-RT-PCR from microarray data using a block bootstrap re-sampling scheme. *BMC Genomics* 8:140.
- Wachi, S., Yoneda, K., and Wu, R. 2005. Interactome-transcriptome analysis reveals the high centrality of genes differentially expressed in lung cancer tissues. *Bioinformatics* 21:4205-4208.

## Ovary

- Hendrix, N.D., Wu, R., Kuick, R., Schwartz, D.R., Fearon, E.R., and Cho, K.R. 2006. Fibroblast growth factor 9 has oncogenic activity and is a downstream target of Wnt signaling in ovarian endometrioid adenocarcinomas. *Cancer Res* 66:1354-1362.
- Lancaster, J.M., Dressman, H.K., Whitaker, R.S., Havrilesky, L., Gray, J., Marks, J.R., Nevins, J.R., and Berchuck, A. 2004. Gene expression patterns that characterize advanced stage serous ovarian cancers. *J Soc Gynecol Investig* 11:51-59.
- Lu, K.H., Patterson, A.P., Wang, L., Marquez, R.T., Atkinson, E.N., Baggerly, K.A., Ramoth, L.R., Rosen, D.G., Liu, J., Hellstrom, I., et al. 2004. Selection of potential markers for epithelial ovarian cancer with gene expression arrays and recursive descent partition analysis. *Clin Cancer Res* 10:3291-3300.
- Welsh, J.B., Zarrinkar, P.P., Sapinoso, L.M., Kern, S.G., Behling, C.A., Monk, B.J., Lockhart, D.J., Burger, R.A., and Hampton, G.M. 2001. Analysis of gene expression profiles in normal and neoplastic ovarian tissue samples identifies candidate molecular markers of epithelial ovarian cancer. *Proc Natl Acad Sci U S A* 98:1176-1181.

## Pancreas

- Buchholz, M., Braun, M., Heidenblut, A., Kestler, H.A., Kloppel, G., Schmiegel, W., Hahn, S.A., Luttges, J., and Gress, T.M. 2005. Transcriptome analysis of microdissected pancreatic intraepithelial neoplastic lesions. *Oncogene* 24:6626-6636.
- Grutzmann, R., Pilarsky, C., Ammerpohl, O., Luttges, J., Bohme, A., Sipos, B., Foerder, M., Alldinger, I., Jahnke, B., Schackert, H.K., et al. 2004. Gene expression profiling of microdissected pancreatic ductal carcinomas using high-density DNA microarrays. *Neoplasia* 6:611-622.
- Iacobuzio-Donahue, C.A., Maitra, A., Olsen, M., Lowe, A.W., van Heek, N.T., Rosty, C., Walter, K., Sato, N., Parker, A., Ashfaq, R., et al. 2003. Exploration of global gene expression patterns in pancreatic adenocarcinoma using cDNA microarrays. *Am J Pathol* 162:1151-1162.
- Ishikawa, M., Yoshida, K., Yamashita, Y., Ota, J., Takada, S., Kisanuki, H., Koinuma, K., Choi, Y.L., Kaneda, R., Iwao, T., et al. 2005. Experimental trial for diagnosis of pancreatic ductal carcinoma based on gene expression profiles of pancreatic ductal cells. *Cancer Sci* 96:387-393.
- Logsdon, C.D., Simeone, D.M., Binkley, C., Arumugam, T., Greenon, J.K., Giordano, T.J., Misek, D.E., Kuick, R., and Hanash, S. 2003. Molecular profiling of pancreatic adenocarcinoma and chronic pancreatitis identifies multiple genes differentially regulated in pancreatic cancer. *Cancer Res* 63:2649-2657.

## Prostate

- Dhanasekaran, S.M., Barrette, T.R., Ghosh, D., Shah, R., Varambally, S., Kurachi, K., Pienta, K.J., Rubin, M.A., and Chinnaiyan, A.M. 2001. Delineation of prognostic biomarkers in prostate cancer. *Nature* 412:822-826.
- Holzbeierlein, J., Lal, P., LaTulippe, E., Smith, A., Satagopan, J., Zhang, L., Ryan, C., Smith, S., Scher, H., Scardino, P., et al. 2004. Gene expression analysis of human prostate carcinoma during hormonal therapy identifies androgen-responsive genes and mechanisms of therapy resistance. *Am J Pathol* 164:217-227.
- Lapointe, J., Li, C., Higgins, J.P., van de Rijn, M., Bair, E., Montgomery, K., Ferrari, M., Egevad, L., Rayford, W., Bergerheim, U., et al. 2004. Gene expression profiling identifies clinically relevant subtypes of prostate cancer. *Proc Natl Acad Sci U S A* 101:811-816.
- LaTulippe, E., Satagopan, J., Smith, A., Scher, H., Scardino, P., Reuter, V., and Gerald, W.L. 2002. Comprehensive gene expression analysis of prostate cancer reveals distinct transcriptional programs associated with metastatic disease. *Cancer Res* 62:4499-4506.
- Liu, P., Ramachandran, S., Ali Seyed, M., Scharer, C.D., Laycock, N., Dalton, W.B., Williams, H., Karanam, S., Datta, M.W., Jaye, D.L., et al. 2006. Sex-determining region Y box 4 is a transforming oncogene in human prostate cancer cells. *Cancer Res* 66:4011-4019.
- Luo, J.H., Yu, Y.P., Cieply, K., Lin, F., Deflavia, P., Dhir, R., Finkelstein, S., Michalopoulos, G., and Becich, M. 2002. Gene expression analysis of prostate cancers. *Mol Carcinog* 33:25-35.

- Magee, J.A., Araki, T., Patil, S., Ehrig, T., True, L., Humphrey, P.A., Catalona, W.J., Watson, M.A., and Milbrandt, J. 2001. Expression profiling reveals hepsin overexpression in prostate cancer. *Cancer Res* 61:5692-5696.
- Nanni, S., Priolo, C., Grasselli, A., D'Eletto, M., Merola, R., Moretti, F., Gallucci, M., De Carli, P., Sentinelli, S., Cianciulli, A.M., et al. 2006. Epithelial-restricted gene profile of primary cultures from human prostate tumors: a molecular approach to predict clinical behavior of prostate cancer. *Mol Cancer Res* 4:79-92.
- Singh, D., Febbo, P.G., Ross, K., Jackson, D.G., Manola, J., Ladd, C., Tamayo, P., Renshaw, A.A., D'Amico, A.V., Richie, J.P., et al. 2002. Gene expression correlates of clinical prostate cancer behavior. *Cancer Cell* 1:203-209.
- Tomlins, S.A., Mehra, R., Rhodes, D.R., Cao, X., Wang, L., Dhanasekaran, S.M., Kalyana-Sundaram, S., Wei, J.T., Rubin, M.A., Pienta, K.J., et al. 2007. Integrative molecular concept modeling of prostate cancer progression. *Nat Genet* 39:41-51.
- Vanaja, D.K., Cheville, J.C., Iturria, S.J., and Young, C.Y. 2003. Transcriptional silencing of zinc finger protein 185 identified by expression profiling is associated with prostate cancer progression. *Cancer Res* 63:3877-3882.
- Varambally, S., Yu, J., Laxman, B., Rhodes, D.R., Mehra, R., Tomlins, S.A., Shah, R.B., Chandran, U., Monzon, F.A., Becich, M.J., et al. 2005. Integrative genomic and proteomic analysis of prostate cancer reveals signatures of metastatic progression. *Cancer Cell* 8:393-406.
- Welsh, J.B., Sapinoso, L.M., Su, A.I., Kern, S.G., Wang-Rodriguez, J., Moskaluk, C.A., Frierson, H.F., Jr., and Hampton, G.M. 2001. Analysis of gene expression identifies candidate markers and pharmacological targets in prostate cancer. *Cancer Res* 61:5974-5978.
- Yu, Y.P., Landsittel, D., Jing, L., Nelson, J., Ren, B., Liu, L., McDonald, C., Thomas, R., Dhir, R., Finkelstein, S., et al. 2004. Gene expression alterations in prostate cancer predicting tumor aggression and preceding development of malignancy. *J Clin Oncol* 22:2790-2799.

### Thyroid

- Huang, Y., Prasad, M., Lemon, W.J., Hampel, H., Wright, F.A., Kornacker, K., LiVolsi, V., Frankel, W., Kloos, R.T., Eng, C., et al. 2001. Gene expression in papillary thyroid carcinoma reveals highly consistent profiles. *Proc Natl Acad Sci U S A* 98:15044-15049.

## Supplementary Figure Legends

**Figure S1.** PINCH1 determines cellular radio- and chemosensitivity in vitro. **(A and B)** Clonogenic cell survival of *PINCH1<sup>fl/fl</sup>*, *PINCH1<sup>-/-</sup>*, EGFP-PINCH1 or EGFP MEF grown on Fibronectin (FN) after irradiation (0 – 6 Gy) or after 1-h Cisplatin treatment (0.1, 1 and 10  $\mu$ M). Results show mean  $\pm$  s.d. ( $n = 3$ ; \*  $P < 0.05$ , \*\*  $P < 0.01$ ; t-test).

**Figure S2.** Tumor allograft identification. **(A and B)** Various excised tumors (#, number of animal) were subjected to PCR genotyping and protein expression (Western blotting) for PINCH1 as described previously in comparison to normal mouse tissues (6).  $\beta$ -actin served as loading control. bp, base pairs.

**Figure S3.** Tumor growth delay and tumor control probability of *PINCH1<sup>fl/fl</sup>* and *PINCH1<sup>-/-</sup>* allografts. **(A)** Accessory tumor volume data sets plotted against time. Comprehensive data sets of tumors irradiated with single doses of 26, 32, 38, 44, 50, 56 or 62 Gy (mean  $\pm$  s.e.m. of 10 - 18 mice). **(B)** Direct comparison of growth characteristics of non-irradiated and 32-Gy irradiated tumors plotted in a semi-logarithmic scale. Median values for the time to grow to 2 and 5 times the starting volume (large symbols) of *PINCH1<sup>fl/fl</sup>* and *PINCH1<sup>-/-</sup>* tumors were compared using the Mann Whitney U test (\*  $P < 0.05$ ) (compare Supplemental Table S2). **(C)** Tumor control probability as a function of radiation dose in *PINCH1<sup>fl/fl</sup>* and *PINCH1<sup>-/-</sup>* tumors growing in immunocompromised mice. Tumor control rates (symbols) were obtained from 11 to 18 animals per dose group. Lines represent tumor control probability for *PINCH1<sup>-/-</sup>* tumors calculated using maximum likelihood analysis. Error bars represent 95% confidence interval of the tumor control dose 50% (TCD<sub>50</sub>). The non-parametric bootstrap method was used to determine 95% confidence intervals for TCD<sub>50</sub>.

**Figure S4.** Assessment of Ki-67-positivity, vasculature, perfusion and hypoxia in *PINCH1<sup>fl/fl</sup>* and *PINCH1<sup>-/-</sup>* allografts. **(A)** Subcutaneous allograft *PINCH1<sup>fl/fl</sup>* and *PINCH1<sup>-/-</sup>* tumors were grown in immunocompromised mice. After tumor formation (diameter 6 - 8 mm), one experimental arm consisted of Pimonidazole and Hoechst 33342 injection at indicated time points prior to tumor excision. **(B)** Haematoxylin and eosin (H&E; panels a, b) or Ki-67 (panels c, d) stained sections of

*PINCH1<sup>fl/fl</sup>* and *PINCH1<sup>-/-</sup>* tumors, respectively, at a tumor diameter of 6 - 8 mm (bars, 50  $\mu$ m). **(C)** Assessment of Ki-67 positive cells among total cells was performed using 10 randomly selected high-power fields (400-fold magnification) per tumor and plotted in percentage scale. Results show mean  $\pm$  s.d.. Statistics compared *PINCH1<sup>fl/fl</sup>* versus *PINCH1<sup>-/-</sup>* tumors using the unpaired, 2-sided t-test (\*  $P < 0.05$ ). **(D)** Representative images of Pimonidazole/Hoechst 33342 co-labeled tumors are shown. According to the experimental design described in A, fixed central whole tumor cross-sections were stained against CD31 and Pimonidazole prior to scanning of fluorescence-labeled cross-sections for Hoechst 33342, TRITC and the FITC fluorescence at 100-fold magnification using a Zeiss Axioplan 2 fluorescence microscope. **(E)** After scanning, image analysis was performed using the KS300 image analysis software. Results show mean  $\pm$  s.d. ( $n = 12$  *PINCH1<sup>fl/fl</sup>*;  $n = 9$  *PINCH1<sup>-/-</sup>*). Statistics comparing *PINCH1<sup>fl/fl</sup>* versus *PINCH1<sup>-/-</sup>* tumors were calculated with an unpaired, 2-sided t-test.

**Figure S5.** PINCH1 regulates Akt1 and FoxO1 phosphorylation. **(A)** Densitometry was performed from data sets presented in Figure 2A and normalized to total expression of corresponding proteins (mean  $\pm$  s.d.;  $n = 3$ ; \*  $P < 0.05$ , \*\*  $P < 0.01$ ; t-test). **(B)** Western blot analysis of total and S9 phosphorylated GSK3 $\beta$ .  $\beta$ -actin served as loading control.

**Figure S6.** PINCH1 determines cellular sensitivity to ionizing radiation and chemotherapeutics in human colorectal carcinoma cell lines. Cells (DLD1, HCT15, HCT116 as indicated) were exposed to 0 - 6 Gy X-rays **(A)** or treated for 1 h with increasing concentrations of Cisplatin **(B)** or 5-FU **(C)** under PINCH1 depletion (P1 siRNA #1, #2; co, non-specific siRNA control). Data show mean  $\pm$  s.d. ( $n = 3$ ; \*  $P < 0.05$ , \* $P < 0.05$ , \*\*  $P < 0.01$ ; t-test).

**Figure S7.** **(A)** Western blot analysis of indicated proteins from DLD1 and HCT15 PINCH1 knockdown cultures (P1 siRNA #1, #2; co, non-specific siRNA control). **(B)** Densitometry was performed from data sets presented in Figure 3E and Figure S7A and normalized to total expression of corresponding proteins (mean  $\pm$  s.d.;  $n = 3$ ; \*\*  $P < 0.01$ ; t-test). **(C)** Western blot analysis of total and S9 phosphorylated GSK3 $\beta$  DLD1 PINCH1 knockdown cultures (P1 siRNA #1, #2; co, non-specific siRNA control).

**Figure S8.** Focal adhesion co-localization of PINCH1, Akt1 and PP1 $\alpha$ . EGFP-PINCH1 and EGFP cells were stained for Akt1 and PP1 $\alpha$  (nuclei stained with DAPI) and confocal images were obtained. Arrows indicate Akt1 or PP1 $\alpha$  in focal adhesions.

**Figure S9.** Titration curves for measurement of protein phosphatase activity. **(A)** Representative curves of protein phosphatase activities of different amounts of cell lysates (0 - 12.5  $\mu$ g) from *PINCH1*<sup>fl/fl</sup>, *PINCH1*<sup>-/-</sup>, EGFP-PINCH1 and EGFP MEF measured according to the manufacturer's protocol. For calculation of data shown in Figure 5F, fluorescence intensities of 0.78  $\mu$ g, 1.56  $\mu$ g, 3.13  $\mu$ g and 6.25  $\mu$ g total protein amounts were used ( $n = 4$ ). **(B)** Western blot analysis of PP1 $\alpha$  expression. **(C)** Representative curves of protein phosphatase activities of different amounts of cell lysates (0 – 6.25  $\mu$ g) from DLD1 control and PINCH1 knockdown cells measured as described in A.

**Supplemental Tables**

**Table S1.** Numbers of animals in the radiation experiment. Data sets for Kaplan-Meier analysis of actuarial estimates for time to local tumor recurrence.

<b>Dose in Gy</b>	<b>Number of animals</b>	
	<b><i>PINCH1<sup>fl/fl</sup></i></b>	<b><i>PINCH1<sup>-/-</sup></i></b>
<b>0</b>	14	14
<b>26</b>	12	12
<b>32</b>	13	12
<b>38</b>	12	14
<b>44</b>	13	14
<b>50</b>	12	18
<b>56</b>	11	14
<b>62</b>	12	15

**Table S2.** Growth of unirradiated and irradiated (32 Gy) *PINCH1<sup>fl/fl</sup>* and *PINCH1<sup>-/-</sup>* tumors in nude mice. Additional data related to Figure S3B. Tumor growth time (TGT) is the time needed after start of experiments to reach 2 and 5 times the starting volume (TGT<sub>V2</sub>, TGT<sub>V5</sub>). SE, standard error.

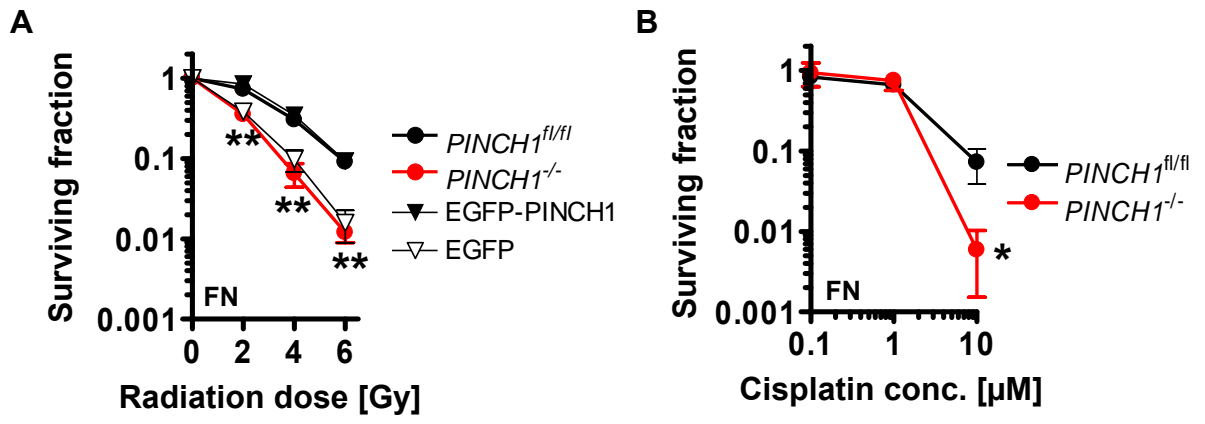
Tumor	Experimental arm	Median TGT <sub>V2</sub> (days) [SE]	P-value for <i>PINCH1<sup>fl/fl</sup></i> vs <i>PINCH1<sup>-/-</sup></i>	Median TGT <sub>V5</sub> (days) [SE]	P-value for <i>PINCH1<sup>fl/fl</sup></i> vs <i>PINCH1<sup>-/-</sup></i>
<i>PINCH1<sup>fl/fl</sup></i>	non-irradiated	1.5 [0.12]	0.01	3.9 [0.32]	0.02
<i>PINCH1<sup>-/-</sup></i>	non-irradiated	1.9 [0.23]		5.0 [0.55]	
<i>PINCH1<sup>fl/fl</sup></i>	32 Gy	19.0 [0.29]	0.01	24.0 [0.58]	0.05
<i>PINCH1<sup>-/-</sup></i>	32 Gy	23.5 [0.58]		27.0 [2.6]	

**Table S3.** Microarray data sets from Oncomine ([www.oncomine.org](http://www.oncomine.org)) for analysis of PINCH1 expression data in tumor tissue versus corresponding normal tissue. References are listed in Supplemental References.

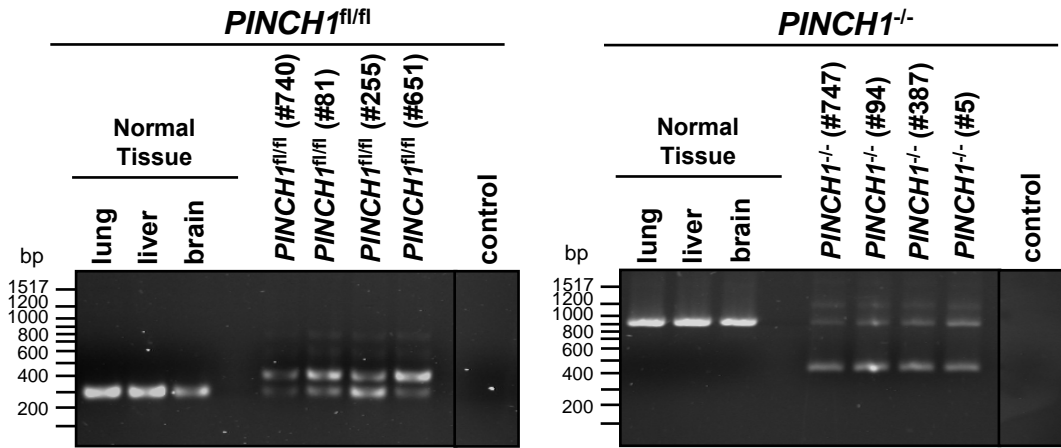
<b>Tissue</b>	<b>No. of studies</b>	<b>Normal</b>	<b>Tumor</b>
<b>Adrenal</b>	1	3	11
<b>Brain</b>	4	37	162
<b>Breast</b>	4	25	143
<b>Colon</b>	4	66	97
<b>Esophagus</b>	3	47	22
<b>Kidney</b>	3	21	44
<b>Lung</b>	7	99	364
<b>Ovary</b>	4	16	196
<b>Pancreas</b>	5	48	68
<b>Prostate</b>	14	189	413
<b>Thyroid</b>	1	8	8
<b>All</b>	<b>50</b>	<b>559</b>	<b>1528</b>

**Table S4.** List of hits identified by mass spectrometry in anti-GFP and anti-Akt1 antibody pulldowns from EGFP-PINCH1 MEF. Hits identified in anti-GFP Ig IP from EGFP MEF served as a control and were excluded from further analysis performed on EGFP-PINCH1 MEF samples.

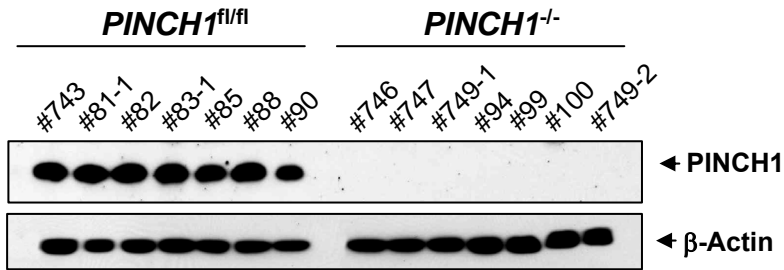
N	Protein accession number	Gene name	anti-GFP Ig		anti-Akt1 Ig	
			Number of matched peptides	Sequence coverage %	Number of matched peptides	Sequence coverage %
1	IPI00130185	PPP1ca	2	10	3	13
2	IPI00876048	PPP1R12A	11	12	4	4
3	IPI00229080	HSP90AB1	6	10	16	25
4	IPI00759925	LIMA1	23	33	17	24
5	IPI00116668	ILK	14	30	-	-
6	IPI00470003	Alpha-Parvin	14	36	-	-
7	IPI00555071	Rsu1	11	38	-	-

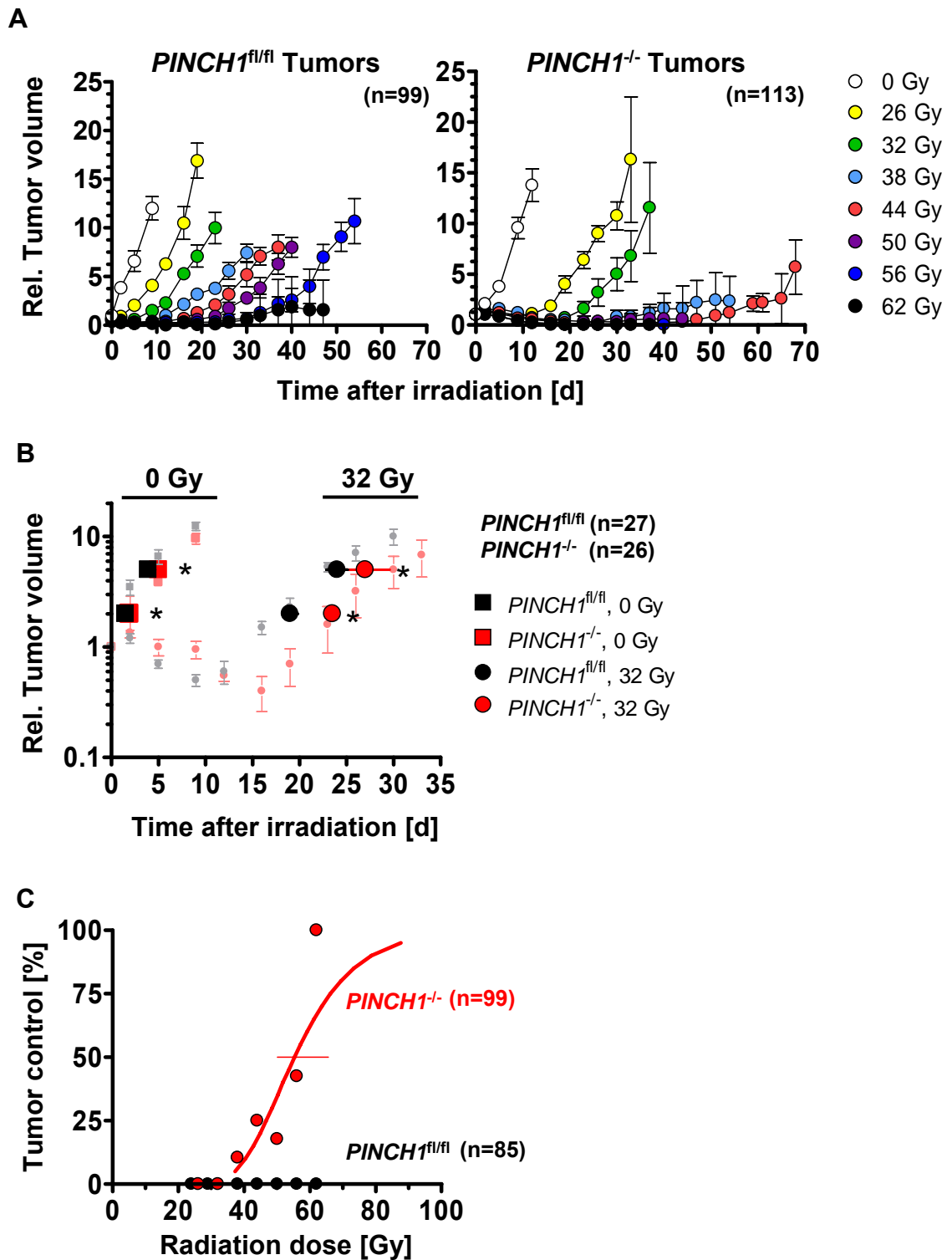


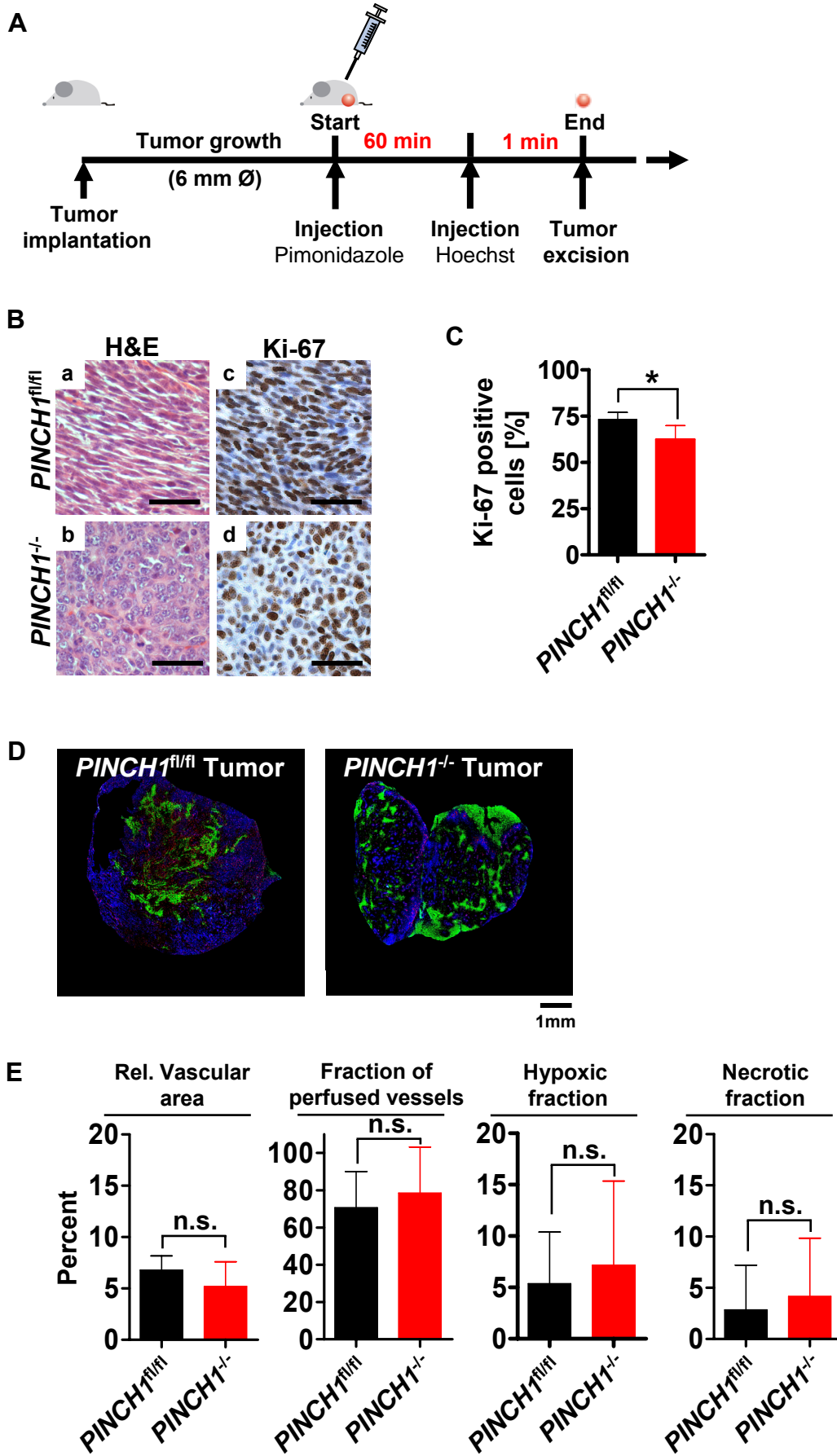
**A**



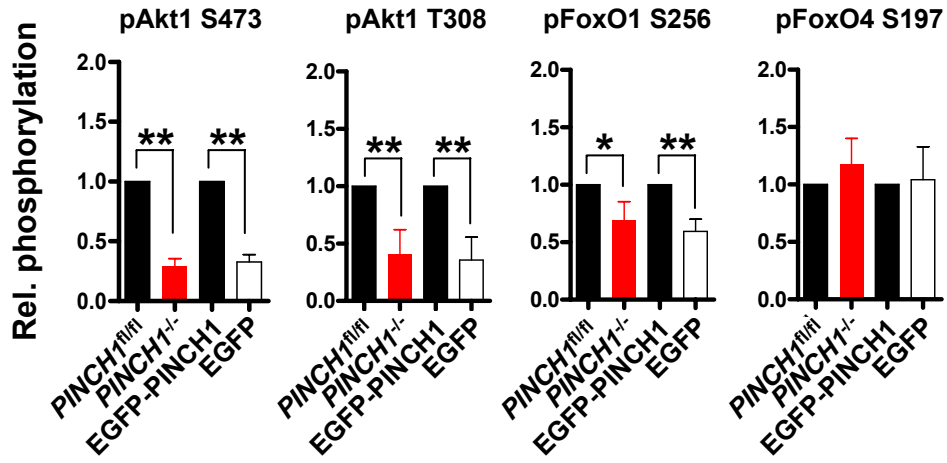
**B**



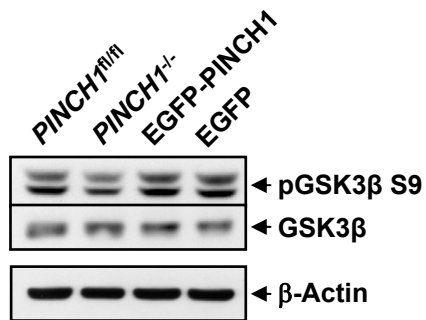


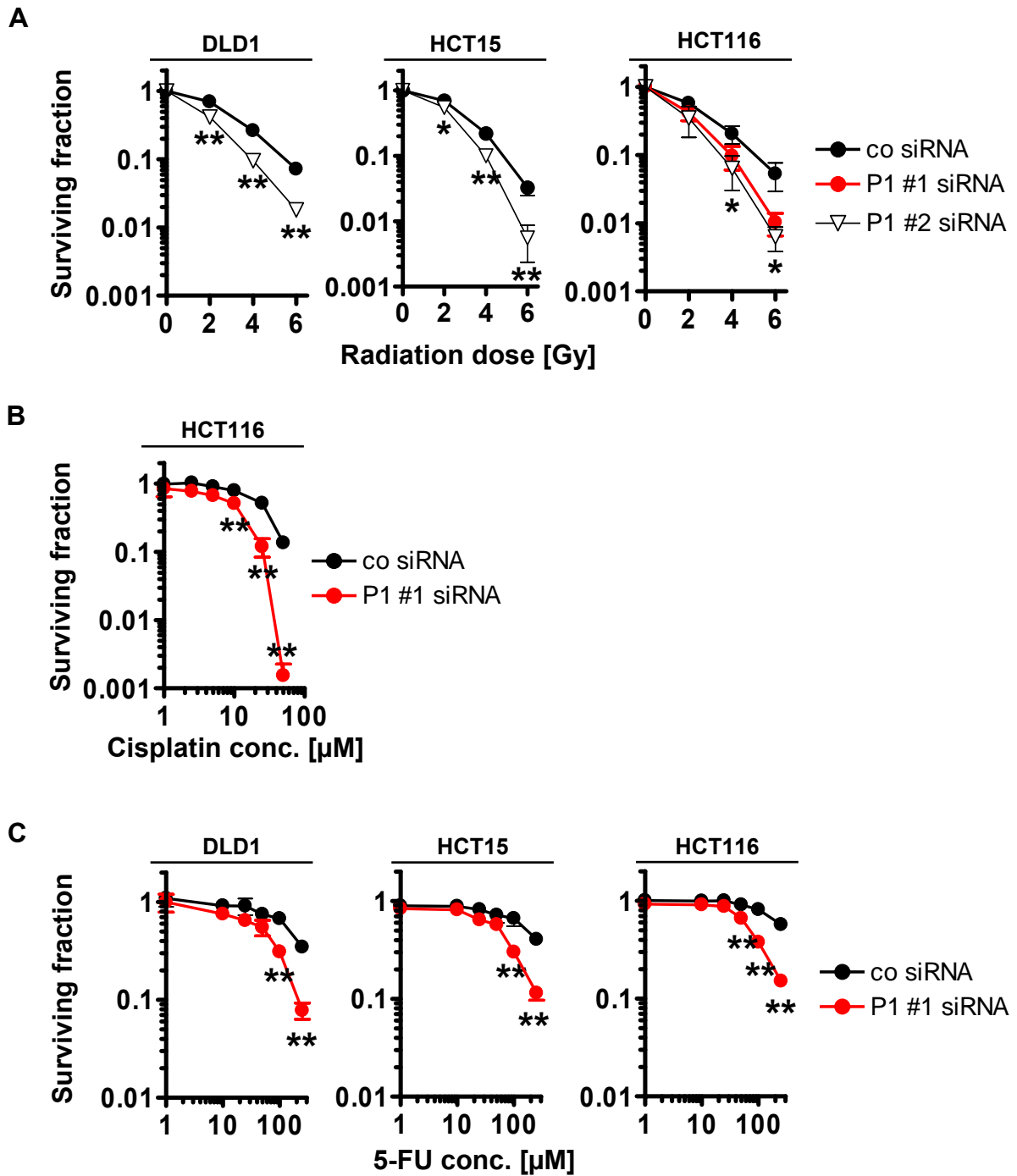


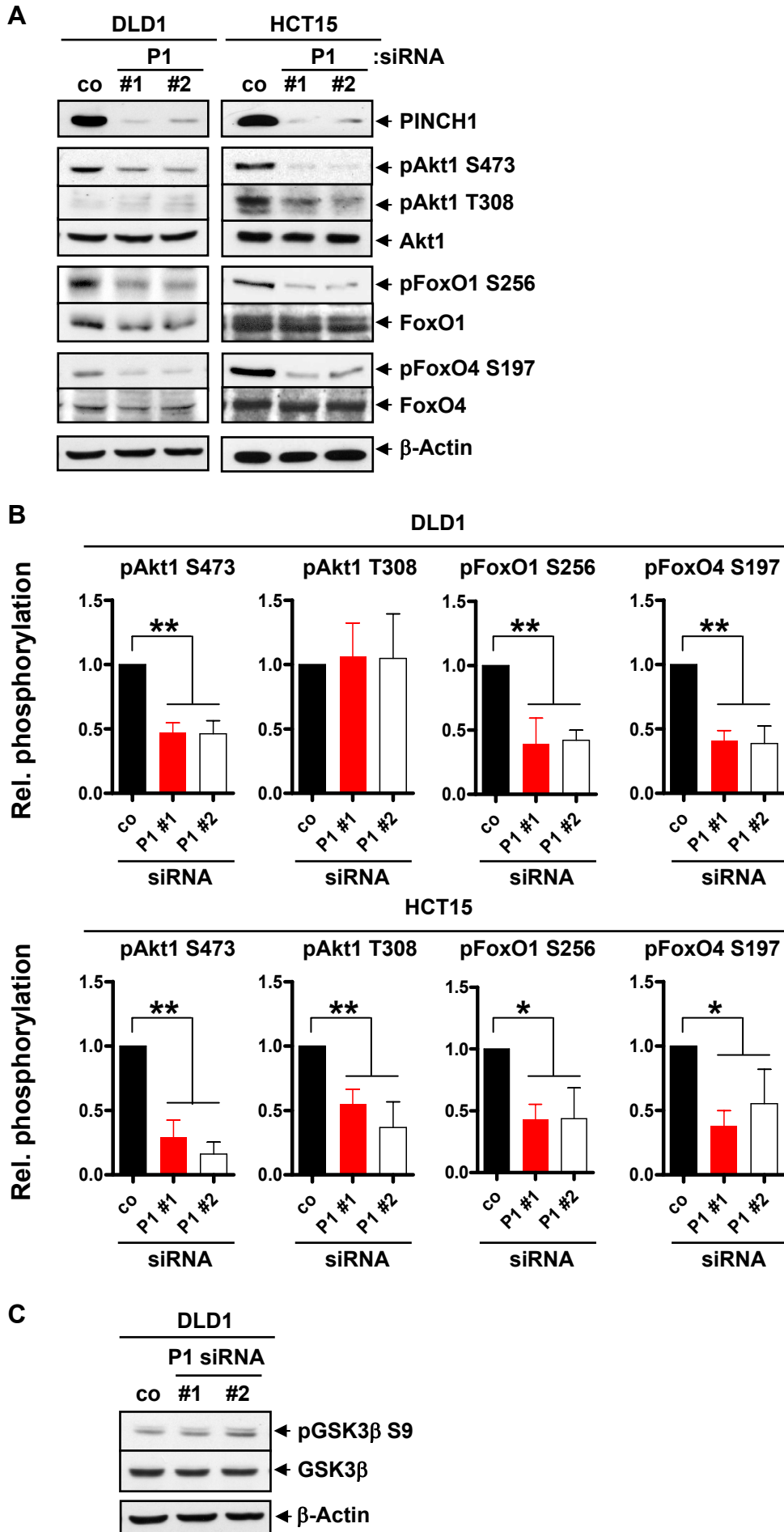
A

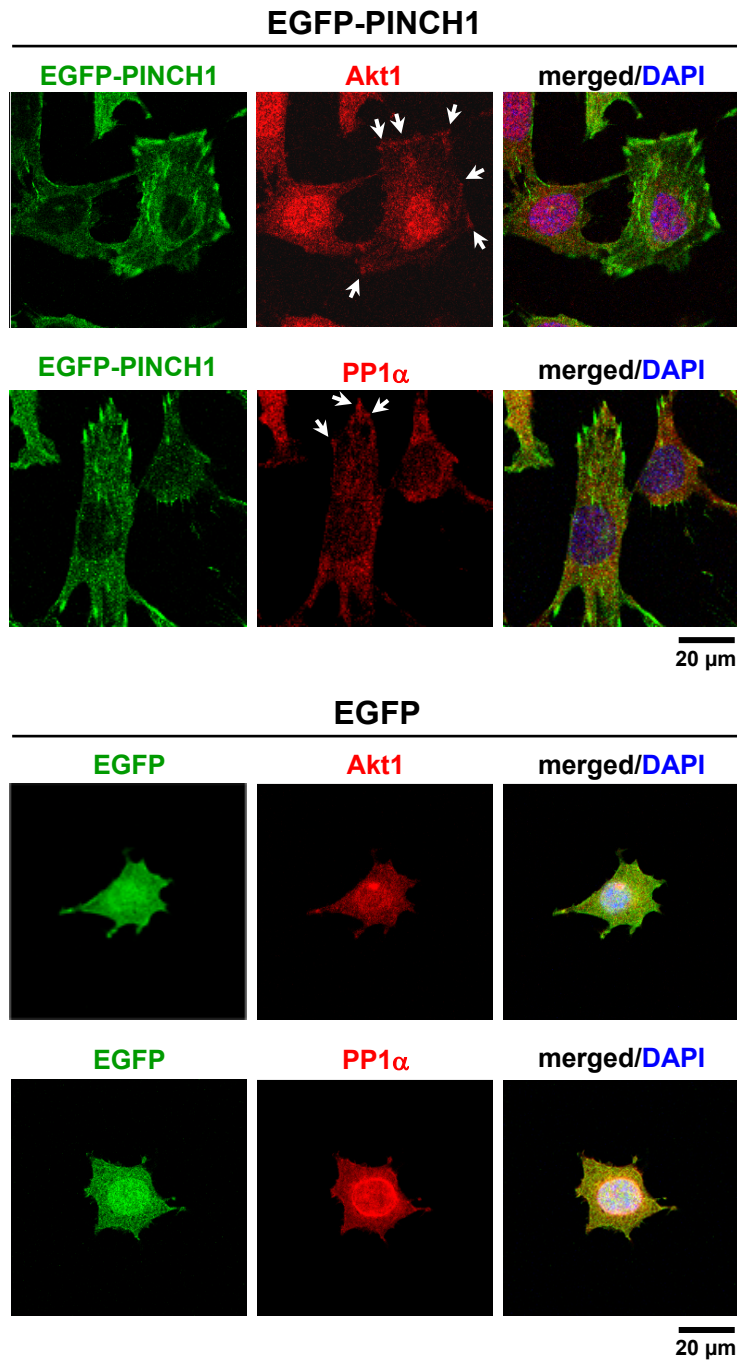


B

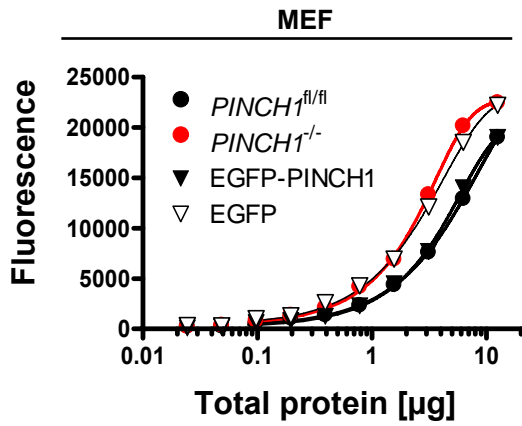




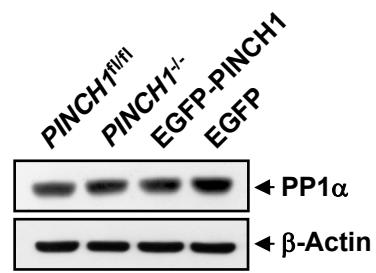




A



B



C

